Large Mammals Have More Powerful Antibacterial Defenses Than Expected from Their Metabolic Rates

Cynthia J. Downs[1], Laura A. Schoenle[2,3], Eric W. Goolsby[4], Samantha J. Oakey[2], Ray Ball[5], Rays H.Y. Jiang[2], Kirk C. Klasing[6], Lynn B. Martin[2]

[1] Department of Environmental Biology, State University of New York College of Environmental Science and Forestry, Syracuse, NY 13210 USA

[2] Global and Planetary Health, University of South Florida, Tampa, FL 33620 USA

[3] Current address: Office of Undergraduate Biology, Cornell University, Ithaca, NY 14853 USA

[4] Department of Biology, University of Central Florida, Orlando, FL 32816 USA

[5] Department of Biology, Eckerd College, Saint Petersburg, FL 33711 USA

[6] Department of Animal Science, University of California, Davis, CA 95616 USA

Short title: Scaling of mammalian antibacterial defenses

Keywords: allometry, antibacterial capacity, constitutive immunity, immune defenses, safety factory hypothesis, scaling

Article type: Major Article

Elements of the manuscript: main text, supplemental materials document (including Supplementary Methods, Figs. S1 to S7, Tables S1 to S6, Captions for Movies S1), and Movie S1

Abstract

Terrestrial mammals span 7 orders of magnitude in body size, ranging from the < 2 g pygmy shrew (*Suncus etruscus*) to the > 3900 kg African elephant (*Loxodonta africana*). Although body size has profound effects on the behavior, physiology, ecology, and evolution of animals, how investment in immune defenses changes with body size is unknown. Here, we develop a novel 12-point dilution-curve approach to describe and compare antibacterial capacity against 3 bacterial species among >160 terrestrial species of mammals. We show that antibacterial activity in serum across mammals exhibits isometry, but the serum of large mammals is less hospitable to bacteria than would be predicted by their metabolic rates. Specifically, hypometric metabolic rates would predict that a large species should have disproportionately lower antibacterial capacity than small species, but body size is unrelated to killing capacity across species. Scaling of antibacterial immune defenses provides novel perspectives on the ecology of host-pathogen interactions, and on their co-evolutionary dynamics. These results have direct implications for effectively modeling the evolution of immune defenses and identifying potential reservoir hosts of zoonotic pathogens.

Introduction

Hosts can be thought of as islands whose size impacts how many parasites, including microbes, can colonize them (Kuris et al. 1980). Bigger hosts represent bigger islands, leading parasite abundance (Kieft and Simmons 2015), biomass (Poulin and George-Nascimento 2007), diversity (Ezenwa 2004), size (Harrison 1915), size diversity (Poulin 2007), and prevalence (Ishtiaq et al. 2017) to increase with host body size. Large-bodied species also appear more susceptible to some parasite infections (Filion et al. 2020). Large body size is also intimately connected to the relative value of self-defense versus reproduction (Calder 1984), as most hosts reach large size via a long lifespan (Harrison 2017; Downs et al. 2020). Altogether, natural selection should favor the evolution of robust immune systems in large hosts (Sheldon and Verhulst 1996; Downs et al. 2014), and despite a few theoretical (Langman and Cohn 1987; Wiegel and Perelson 2004; Banerjee et al. 2017) and empirical (Lee 2006; Schoenle et al. 2018) calls to investigate scaling of immune defenses, very little works has yet considered whether and how immune defenses scale across the full range of terrestrial mammalian body sizes.

Generally, body size scaling relationships are modeled as power laws, $Y = a\,M^b$, with linear transformations, $\log_{10} Y = \log_{10} a + b \log_{10} M$, where Y is the focal trait, M is body mass, a is the intercept, and b is the scaling factor. Four hypotheses make predictions about the values of the scaling factors describing the relationship between immune defenses and body mass. To date, the Protecton and the Complexity of Immunity Hypotheses have received the most attention. Both hypotheses predict that immunity should scale in direct proportion to body size (i.e., isometrically), which results in a mass-invariant relationship ($b = 0$) for concentrations (Langman and Cohn 1987; Wiegel and Perelson 2004). The fractal nature of the circulatory and lymphatic systems is argued to predict isometry because rates of parasite detection and delivery

of defenses should be driven by transit of cells and proteins through the vasculature (e.g., Wiegel and Perelson 2004; Banerjee et al. 2017; Banerjee 2018). Although this framework was developed for predicting the number of a single clone of B cells necessary to detect an antigen in a host and circulation time of a B cell (Wiegel and Perelson 2004), it has been extended to make predictions about other types of immune defenses but particularly adaptive immunity (Banerjee et al. 2017; Banerjee 2018). By contrast, the Rate of Metabolism Hypothesis predicts a hypometric coefficient for immunity ($b < 0$) because all cellular activities are linked to basal metabolic rates (BMR) (Brown et al. 2004). As mass-specific BMR scales at $b = -0.25$, immune defenses involving cell turnover and metabolism should scale similarly (Dingli and Pacheco 2006).

Finally, the Safety Factor Hypothesis invokes performance-safety relationships from biophysics (Harrison 2017) and physiology (Diamond 2002), and posits that large species should evolve disproportionately stronger (i.e., hypermetric, $b > 0$) damage-mitigation mechanisms than small ones (Harrison 2017; Downs et al. 2020). Immunologically, the Safety Factor Hypothesis predicts that large hosts should evolve exceptionally robust constitutive defenses to protect against the greater infection risks they will experience. Variants of the Safety Factor Hypothesis exist in the literature already, including Peto's paradox for cancer (Peto 1977) and optimal defense theory (Shudo and Iwasa 2001). Only recently, however, has direct empirical evidence been provided for immune defenses, namely hypermetric scaling for both neutrophil concentrations in mammals ($b = 0.11$) (Downs et al. 2020) and heterophil concentrations in birds ($b = 0.19$) (Ruhs et al. 2020).

Despite evidence for some immune allometries, it remains obscure whether the functional capacity of immune defenses scale similarly. Does hypermetric scaling of granulocyte

85 concentrations represent greater immune protection in large animals or simply evidence that
86 large animals must compensate for lower per-granulocyte effectiveness by circulating more
87 cells? Cell size scales isometrically with body mass, but per-gram metabolism scales
88 hypometrically (Schmidt-Nielsen 1984), so the average large-animal leukocyte might be
89 comparatively ineffective compared to a leukocyte from a small species. Moreover, as selection
90 tends to act on integrated traits (Bennett and Huey 1990), scaling inference based on processes
91 that affect host fitness (i.e., control of bacterial infections) will inherently be more insightful than
92 studies solely based on cell concentrations. Few scaling studies of immunity to date have relied
93 on integrated immune functions, and others either involved few species, narrow taxonomic
94 groups, or found body mass effects but did not estimate allometries (e.g., Nunn 2002; Blount et
95 al. 2003; Nunn et al. 2003; Lee et al. 2008; Schneeberger et al. 2013; Tian et al. 2015;
96 Fassbinder-Orth et al. 2019; reviewed in Downs et al. 2020).

97 Our goals here were i) to determine how blood-based antibacterial defenses scaled with
98 body size among terrestrial mammals, and ii) to test which hypothesis best-predicts the scaling
99 exponent (*b*) for this type of immunity. We focused on antibacterial capacity of sera (French and
100 Neuman-Lee 2012), as this defense is functional and integrative (Demas et al. 2011), is an
101 important determinant of host health and virulence for certain bacterial pathogens (Taylor 1983),
102 and is measurable in a standard, reagent-independent way. Briefly, antibacterial capacity
103 measures bacteriostasis and bacteria killing capacity of sera. To describe interspecific variation
104 in this immune function in the most confound-free manner possible, we compared the efficacy of
105 sera of several, independent replicates from adults of mammalian species housed in zoos. To
106 provide generality to any scaling we observed, we quantified the antibacterial capacity of sera of
107 160+ mammalian species against three distinct bacteria, *Escherichia coli* (ATCC #8739),

108 *Salmonella enterica* (ATCC #13311), and *Micrococcus luteus* (ATCC # 4698). These bacteria
109 are common pathogens of many vertebrates (Mastroeni et al. 2001), some portion of their natural
110 infection timeline occurs in blood (Mittrücker and Kaufmann 2000), and they are controlled
111 effectively by blood-borne immune defenses (Taylor 1983). As the last common evolutionary
112 ancestor of our focal microbes was ancient, any consistency in allometries should be more
113 attributable to host immunity than parasite evolutionary history.

114 To enable meaningful comparisons across species, we characterized antibacterial dilution
115 series, instead of antibacterial capacity at single dilutions (as is typically used, French and
116 Neuman-Lee 2012), as the shapes of resultant *ex vivo* antibacterial functions capture salient
117 aspects of defense (Fig. 1A). For instance, if a very dilute serum sample was effective against a
118 standard amount of bacteria, a given individual of that host species would be relatively adept at
119 controlling a large initial dose of bacteria in its bloodstream. Other meaningful antibacterial
120 parameters included i) the maximum amount of bacteria that serum could protect against, ii) the
121 serum dilution at the point of most rapid change from protected to vulnerable, and iii) the slope
122 at this steepest part of the antibacterial function (Fig. 1A). This last parameter could be a proxy
123 for either how rapidly serum defenses could be recruited to a bacterial replication event (Murphy
124 et al. 2007) or capture the pattern by which proteins and other molecules were recruited
125 combinatorically to control bacteria. The Safety Factor Hypothesis, our focal hypothesis, predicts
126 that large mammals will have disproportionately higher maximal antibacterial capacity, higher
127 antibacterial capacity at a specific dilution, and a more rapid shift from vulnerable to complete
128 protection than small species (Fig. 1B). By contrast, the Rate of Metabolism Hypothesis predicts
129 the opposite for large mammals relative to small ones (Fig 1C), and the Protecton and

130 Complexity Hypotheses predict that large mammals will have the same antibacterial capacity as
131 small species (Fig. 1D).
132

133 Materials and Methods

134 Samples

135 We used the simulations performed by Dingemanse and Dochtermann (Fig. 1 of 2013) to
136 guide our sample sizes. We obtained serum from healthy, zoo- and lab-housed animals ranging
137 in body size from 16 g – 3,600 kg, which covers the range of body sizes of extant terrestrial
138 mammals (Fig. S1) (Smith and Lyons 2011). We supplemented these samples, which comprised
139 the vast majority of our sample, with those from lab-housed animals to augment the small-bodied
140 species (< 2 kg) included in our analysis, as these body sizes are rare for mammals in most zoos.
141 Most zoo samples were collected as part of routine wellness checkups whereas lab samples were
142 collected at the termination of experiments; all animals from which samples were taken were
143 outwardly healthy. We could not run all assays against all bacterial species for all samples
144 because of sample volume constraints. Final sample sizes of mammal species were 199, 186, and
145 164 for antibacterial capacity against *E. coli, S. enterica,* and *M. luteus*, respectively. We assayed
146 a mean of ≥ 4 samples per species for each microbe (n = 1-41 replicates per species, Fig. S2). We
147 also obtained >15 samples from a subset of species representing the full range of body masses to
148 ensure that a single individual from a large or small species was not biasing a species mean (Fig.
149 S3). Samples were stored at the collection location at -80 to -20 °C until shipped on dry ice to
150 our research labs where they were stored at 80 °C until assays. Samples were used in assays
151 within 24h of thawing. We restricted our analysis to samples collected in the years 2005-2019
152 because preliminary work indicated that older samples had reduced antibacterial ability. Use of

153 these samples was approved by the Institutional Animal Care and Use Committees at home
154 institutions. Samples were collected as part of routine veterinary exams under auspices of zoo
155 IACUCs and were shared after approval by the appropriate committee at each zoo.
156

157 **Antibacterial capacity**

158 We measured antibacterial capacity against *E. coli* (ATCC #8739), *S. enterica* (ATCC
159 #13311), and *M. luteus* (ATCC # 4698) using an adaptation of the microbiocidal assay (a.k.a.
160 bacteria killing assay, BKA, microbiocidal activity) developed by French and Neuman-Lee
161 (2012). Briefly, we plated a 12-point dilution curve of each serum sample in triplicate on a
162 round-bottomed 96-well plate. *E. coli* had two serial dilutions: 6 points from undiluted serum to
163 1:64, and 6 points from 3:4 to 3:256. *S. enterica* also had two serial dilutions: 6 points from
164 undiluted to 1:64, and 6 points from 3:4 to 3:128. *M. luteus* had a single serial dilution ranging
165 from undiluted serum to 1:2048. Super antibacterial capacity curves—curves for species with
166 100% antibacterial capacity at the lowest dilution of the normal curves—for *E. coli* were 6 points
167 from 1:4 to 1:256 and 6 points from 3:16 to 3:512 and for were *S. enterica*: 6 points from 1:16 to
168 1:512 and 6 points from 3:4 to 3:128. We also plated a 4-point dilution curve in Dulbecco's
169 Phosphate Buffered Saline (PBS, Sigma-Aldrich #D8537) of commercially available cow serum
170 (Innovative Research Novi, MI 48377, #IBV-Compl) as our inter-assay control. Cow curve
171 dilutions were 1:32, 1:64, 1:128, 1:256 for *E. coli*; 1:16, 1:32, 1:64, 1:128 for *S. enterica*; and
172 1;20, 1:80, 1:320, 1:1280 for *M. luteus*. Our final volume of each serum dilution was 18 µl. We
173 plated three replicates of a 20 µl negative control of PBS and 9 replicates of an 18 µl positive
174 control. We added 2 µl of a standard concentration (10^4 CFU ml^{-1}) of bacteria to all wells except
175 the negative controls. We incubated plates for 30 min at 37 °C. We next added 125 µl of tryptic

soy broth (BD #211825) to all wells, and then shook plates for 1 min at 300 rpm. We then measured baseline absorbance of all wells at 300 nm (Biotek Synergy HTX Multi-Mode Reader) to serve as an internal control before incubating covered plates for 12 h for *E. coli*, 10 h for *S. enterica*, and 48 h for *M. luteus* at an incubation temperature of 37 °C. We then measured final absorbance of all wells again at 300 nm and calculated antibacterial capacity for each well as $\left(1 - \frac{mean(sample\ end - sample\ baseline)}{mean(positive\ control\ start - positive\ control\ end)}\right) * 100\%$. Inter-assay (9.02%) and intra-assay variation (0.02%) were both low. Key parameters of the antibacterial capacity assay for each microbe are summarized in Table S1 and full details about the procedures used to develop and validate our assays are available in the Supplementary Methods. Assay protocols are deposited on FigShare (Schoenle et al. 2020).

Data processing and analysis

All data processing and analyses were performed in the statistical programming language R (R Core Team 2019). We compiled data using a workflow developed using R (all code files are available on Figshare (Keith et al. 2020; Downs et al. 2021)). We visually checked each sample dilution curve for outliers (i.e., replicates that were distinct from the other two replicates and/or fell off the expected sigmoidal curve). We determined whether positive controls, negative controls, and inter-assay controls (i.e., cow sera) were within the expected range, and discarded a plate if data fell outside expected ranges and reran samples.

To identify any allometries, we first fit non-linear antibacterial functions for each individual sample separately. Properly estimating allometries required models that allowed us to perform phylogenetically multivariate regressions while accounting for the sampling of numerous individuals within a species because we know that species are not independent

samples (Felsenstein 1985) and a failure to account for within-species variation can produce inaccurate regression estimates (Garamszegi and Møller 2010; Garamszegi 2014). This modeling framework is under-served by the available statistical packages, so we modeled data using two main approaches. For our first approach, we used multivariate phylogenetic comparative analyses of our data using the R package `Rphylopars` (Goolsby et al. 2021). This approach allowed us to calculate phylogenetic covariances of traits among species while accounting for numerous observations within a species (i.e., among-individual variation) (Goolsby et al. 2017). Although this approach did not estimate scaling coefficients as they would be estimated with a regression/linear model-based approach, it allowed us to estimate phylogenetic signal of antibacterial capacity and correlations among the antibacterial curve parameters and between curve parameters and body mass in the same model. For our second approach, we built multivariate general linear mixed models using the R package `MCMCglmm` (de Villemereuil and Nakagawa 2014). Although these models assume each species is an independent point, they allowed us to estimate *b* for all curve parameters simultaneously while accounting for the variance within species by including multiple observations per species variation (Dingemanse and Dochtermann 2013). This approach better parallels the traditional approach to estimating scaling coefficients using regression models (Sieg et al. 2009). To test for the strength of phylogenetic signals in a framework based on general linear models, we built phylogenetic univariate general linear mixed models for each antibacterial curve parameter individually using `MCMCglmm` (supplementary methods) (de Villemereuil and Nakagawa 2014). We extracted species relatedness from a tree build using PhyloT (Letunic 2015, Fig S4)

221 Fitting non-linear curves for each individual. For the first step, we fit 5-parameter logistic
222 regression growth curves to each individual antibacterial curve (i.e., the shape of dilution curves
223 across all 12-serum concentrations) using package `nplr` (Commo and Bot 2016) (Fig. 1A). To
224 aid in curve-fitting, we $\log_{10}$-transformed serum concentrations (i.e., the dilutions) and converted
225 the antibacterial ability from a percent to a proportion. Curves could only be fit to values
226 between 0 and 1. So percent inhibited values > 100 were forced to a random value between 99
227 and 100 and percent inhibited values < 0 were forced to a random value between 0 and 1 before
228 conversion to proportions. This approach restricted values to a range near maximal and minimal
229 antibacterial activity for all other curves. We extracted the curve parameters ($\text{inflection}_{\text{dilution}}$,
230 $\text{inflection}_{\text{antibacterial capacity}}$, bottom asymptote, top asymptote, slope, asymptote coefficient) to use in
231 univariate and multivariate general linear models (Fig. 1A). Slope and $\text{inflection}_{\text{dilution}}$ were
232 already on a $\log_{10}$-scale. We added 1 to $\text{inflection}_{\text{antibacterial capacity}}$, bottom asymptote, top asymptote
233 and then $\log_{10}$-transfromed them. We also $\log_{10}$-transformed body mass. All analyses were
234 performed using transformed data.

235 Phylogenetic covariance. We performed a multivariate phylogenetic comparative analysis
236 for antibacterial capacity against each microbe using the R package `Rphylopars` (Goolsby et
237 al. 2021). All antibacterial capacity curve parameters and body mass were included as response
238 variables in these models, with one exception. Top asymptote was not included in the model for
239 antibacterial capacity against *S. enterica* because it was highly correlated (r = 0.998) with
240 $\text{Inflection}_{\text{antibacterial capacity}}$; both could not be included in the same model. We included
241 phylogenetic effects from a tree we produced by pruning the time-rooted phylogenetic tree
242 created by Uyeda et al. (2017) to our species list; we scaled tree with height scaled to 1. Models
243 were fit assuming a Brownian motion model of evolution and we estimated the percent of

variance explained by phylogeny. We tested for phylogenetic signal for each trait using a likelihood ratio test (df = 1) to compare Pagel's lambda against a null model with a star phylogeny (lambda = 0) to our model that included phylogeny (Pagel 1997, 1999).

Multivariate mixed models. We generated separate multivariate mixed models to query body mass effects on antibacterial capacity, one for each bacterial species. All curve parameters were included as response variables, and we allowed each parameter to have different slopes and intercepts. Body mass was included as a fixed effect, and species was incorporated as a random effect. Species had independent intercepts and slopes. These models were fit using the `MCMCglmm` package (Hadfield 2010; Hadfield and Nakagawa 2010; de Villemereuil and Nakagawa 2014). All mixed models were fit using a weak inverse-Gamma prior with shape and scale parameters set to 1.002 for the random effect. Default priors for all other fixed effects were used. Model chains were run for 1.82×10^6 iterations, a 420,000-iteration burn-in, and a 1400 iteration thinning interval. Results were robust across alternative priors, and chain length was sufficient to yield negligible autocorrelation. We extracted the slopes describing the relationship between each parameter and body mass across all species.

We included bacterial capacity at the bottom asymptote and asymmetric coefficient in our models because they helped describe antibacterial capacity curves, although we did not make predictions about their biological functions. In our study, we did not always collect data at the lower asymptote because we limited our sampling to 12-dilutions. As a result, the bottom asymptote estimated by the general linear model was based on incomplete data and not biologically relevant to our scaling hypotheses. The dilution at the inflection point was also included in our models because it informed our understanding of the antibacterial capacity at the

266 inflection point, but it was not obviously biologically meaningful for understanding immune
267 scaling.
268

269 Results

270 Overall results from all three modeling approaches were consistent and supported
271 isometric (i.e., mass-invariant) scaling (*b*=0) for almost all curve parameters for antibacterial
272 capacity parameters against all three microbes. The one exception to this pattern was the slope
273 for antibacterial capacity against *M. luteus*; in this one instance, all three modeling approaches
274 indicated a negative relationship between slope at the intercept with body mass such that slopes
275 become less steeply positive with body mass.

276 Phylogenetic covariance. Models built using `Rphylopars` estimated that the covariance
277 between body mass and any of the curve parameters was very close to zero and had 95% CI
278 intervals that overlapped zero, with one exception (Table 1): the correlation between slope and
279 body mass for antibacterial capacity against *M. leuteus* had a negative correlation of –11.0 (95%
280 CI: -22.8 : -2.6). Lambda values provided evidence of phylogenetic signal in body mass and at
281 least one curve parameter for antibacterial capacity against all three microbes (Table 2).
282 Phylogeny explained >97% for variation in body mass, but only ≤ 30% of the variation in most
283 of the antibacterial capacity curve parameters (Table 2). An exception was that phylogeny
284 explained 54% if of the variation in $\text{Inflection}_{\text{dilution}}$ for antibacterial capacity against *S. enterica*.
285 Phylogenetic correlations among curve parameters and phylotypic correlations can be found in
286 Tables S1 and S2, respectively. These models had slightly smaller sample sizes because not all
287 species were in the time-rooted tree. Final sample sizes of species for these models were 191,
288 178, and 157 for antibacterial capacity against *E. coli, S. enterica,* and *M. luteus*, respectively

289 Phylogenetic univariate mixed effects models. Phylogenetic univariate models supported
290 scaling coefficients of zero. The 95% CI for all curve parameters for antibacterial capacity
291 against *E. coli, S. enterica, M. luteus* overlapped zero except for slope of antibacterial curves
292 against *M. luteus* (supplemental materials, Table S3). This parameter scaled hypometerically (-
293 4.30, 95% CI: -8.34, -0.30). Phylogeny explained 1-18% of the variation in antibacterial curve
294 parameters (supplemental materials, Table S4).
295 Multivariate mixed effects models. Multivariate models supported scaling coefficients of
296 zero for all curve parameters for antibacterial capacity against *E. coli, S. enterica, M. luteus* with
297 two exceptions (Table 3, Fig. 2) The slope of antibacterial curves against *M. luteus* had a
298 hypermetric slope of -4.3 (95% CI: -7.7 : -0.79) and the asymmetric coefficient scaled with a
299 slope of -3.78 (95% CI: -5.604 : -0.91).
300

301 **Discussion**

302 Our data provide consistent and robust evidence for isometric (i.e., mass-invariant)
303 scaling of serum antibacterial activity in terrestrial mammals. Additionally, results indicate that
304 phylogenic signal was surprisingly low for all three microbes. Superficially, isometric scaling
305 supports the prediction of the Protection and Complexity Hypotheses. These results were
306 somewhat surprising, given that large species face a greater risk of infection and face greater lost
307 fitness costs from infections (Downs et al. 2020). Below we argue that the interpretation of these
308 results might support a more complex interpretation once integrated with our understanding of
309 how host metabolic rates and other immunological defenses scale.
310 Mass-invariance of antibacterial capacity was consistent regardless of the bacterial
311 species studied. This discovery is interesting in light of the ecology and life history differences

312 among bacterial species. *M. luteus* grows slowly and causes modest disease in most hosts relative
313 to the other two bacteria; both *S. enterica* and *E. coli* can cause sepsis (van der Poll and Opal
314 2008), infect via the diet, and have similar replication rates in culture. Our findings thus support
315 the idea that broadly effective, fast-acting immune responses are generally favored, rather than
316 by a specific pathogenetic target, across mammalian species.
317
318 Isometric scaling and the Protecton/Complexity Hypotheses
319 Both of the Protecton and Complexity Hypotheses hypotheses argue that large and small
320 animals need equal defenses against parasites, resulting in immune responses having a scaling
321 exponent of 0 (Langman and Cohn 1987; Wiegel and Perelson 2004; Banerjee and Moses 2010).
322 Our results are consistant with this prediction. However, by definition, isometric scaling is
323 difficult to test because it corresponds with a null model of a mass-invariant or intercept-only
324 model. Statistically, we cannot distinguish between the null and the model prediction.
325 Perhaps more importantly, both the Protecton and Complexity Hypotheses were
326 developed to predict how the number of lymphocyte clones should scale with body size to
327 provide protection against foreign antigens (Langman and Cohn 1987; Wiegel and Perelson
328 2004; Banerjee and Moses 2010), not to explain constitutive, innate immunity as studied here.
329 Assumptions about the distribution and timing of adaptive immune responses are unlikely to
330 hold for the early-acting, constitutive innate immune responses. The adaptive and innate immune
331 systems operate on different time scales (Murphy et al. 2007), and the life cycles of lymphocytes
332 and neutrophils are quite different. Circulating peripheral neutrophils have a lifespan of 1-7 days
333 (Hidalgo et al. 2018) whereas peripheral, naïve lymphocytes are long lived—T cells live on the
334 order of years and B cells have a half-life of 4 weeks to several months—and later phases of

335 adaptive immunity (i.e., memory) are controlled by even longer-lived lymphocytes (Tough and
336 Sprent 1995). Even "short-lived" lymphocytes involved in early stages of memory have life-
337 spans of weeks, which is much longer than neutrophils (Tough and Sprent 1995). Although the
338 Complexity Hypothesis has been extended to make predictions about the size and number of
339 lymph nodes in mammals (Banerjee 2018) and host capacity to replicate West Nile virus
340 (Banerjee and Moses 2009, 2010; Banerjee et al. 2017), these extensions are still primarily based
341 on the dynamics of adaptive immunity. It follows that the underpinning logic of the Complexity
342 Hypothesis would need to be rederived from first principles to account for dynamics of innate
343 immune defense and to make predictions for early, broadly active defenses that are part of the
344 innate immune system, such as antibacterial capacity.
345
346 Isometric scaling is steeper than expected by metabolic rates

347 The mass-invariance of antibacterial capacity is intriguing when considered with the
348 well-documented hypometric scaling of mass-specific metabolic rates (Brown et al. 2004;
349 Savage et al. 2004) and the hypermetric scaling of concentrations of some immune cell types
350 (Downs et al. 2020). The Metabolic Theory of Ecology posits that mass-specific metabolic rate
351 can be interpreted as the ratio of the average metabolic rate of a cell to the average cell volume,
352 and this ratio also has a scaling exponent of -0.25 (Savage et al. 2007):

353 $$\frac{metabolic\ rate}{body\ mass} = \frac{mean\ cellular\ metabolic\ rate}{mean\ cell\ volume} \propto body\ mass^{-0.25}.$$

354 If cellular metabolic rate increases, cell volume must decrease (Savage et al. 2007). Thus, for cell
355 types with mass-invariant volumes (b = 0), cellular metabolic rate will scale with the same slope
356 as mass-specific metabolic rate (b = -0.25). It follows that if basal metabolic rate is the

357 pacemaker for cellular activity, protein synthesis for these cell types would also scale with a
358 slope of -0.25 (Brown et al. 2004).

359 Our assay measured the functional capacity of complement and other circulating proteins
360 (i.e., lysozyme, mannan-binding protein, beta-defensins) to opsonize and lyse bacteria (Demas et
361 al. 2011; French and Neuman-Lee 2012). Complement proteins are predominantly produced by
362 hepatocytes (Lubbers et al. 2017), and hepatocyte volume is mass-invariant (Savage et al. 2007).
363 As such, production of complement protein production per hepatocyte should scale at -0.25.
364 Liver mass scales with a slope of 0.895 (Prothero 2015), so. if each hepatocyte produces
365 complement proteins at the same rate, antibacterial capacity should scale at 0.645 (= 0.895-0.25).
366 Within this framework, a scaling coefficient of 0 for antibacterial capacity, as we described, is
367 shockingly high. In other words, large mammals have much higher antibacterial capacity than
368 expected by their metabolic rate alone. An outstanding question is how large mammalian species
369 obtain the same antibacterial capacity as small ones if they are constrained by their metabolic
370 rates.

371 Why isometric scaling?

372 Antibacterial capacity and neutrophil concentrations, the other type of first, constitutive
373 lines of host defense thus far studied in an allometric context (b = 0.11; Downs et al. 2020), both
374 scaling more steeply than expected by scaling of metabolic rates. These scaling repationships
375 may have evolved because, relative to small mammals, large mammals (1) have a
376 disproportionately higher exposure to parasites and (2) have a disproportionately larger gap in
377 replication rates relative to invading microbes (Downs et al. 2020). We will walk through each in
378 turn.

379 First, large mammals have different exposure risks to parasites because of their ecology.
380 Relative to small mammals, large mammals consume more food (Nagy 2001; Nunn et al. 2003),
381 move farther and thus are exposed to more of habitat with each unit of movement (e.g., step,
382 wing flap) (Schmidt-Nielsen 1984), and they have larger home ranges which exposes them to
383 more types of habitats (Lindstedt et al. 1986; Kelt and Van Vuren 2001). Although a given gram
384 of tissue in a large host is less exposed to parasites because of a low ratio of surface area to
385 volume, absolute exposure to parasites is probably much higher in large than small species
386 (Dobson and Hudson 1986; Downs et al. 2019). Large mammals also have a higher absolute
387 exposure to parasites over their lifetime because they have longer lifespans than small mammals
388 (Peters 1983; Calder 1984).

389 Second, parasites have an evolutionary advantage over hosts because of differences in
390 replication rates. When parasites grow rapidly, as bacterial (and viral) infections often do,
391 defenses with short time-delays are favored (Shudo and Iwasa 2001). Barriers against all-comers
392 are the best option when adversaries can replicate faster than defenses can be honed and
393 mobilized. The downside to these forms of defense is that they impose comparatively high costs,
394 especially when adversaries are absent (Sears et al. 2006). Recently, a meta-analysis revealed
395 that small animal species that are relatively long-lived incur the highest costs of *induced* immune
396 defenses (Brace et al. 2017). Given the tendency of small species to breed prolifically and
397 develop rapidly, isometric allometries might manifest as much because small species favor
398 rapidly-mobilizable defenses that are activated only after exposure to a parasite as they do
399 because of mandates of large size.

400 Our understanding of how activation of adaptive immune responses occurs would also
401 support the need for large animals to have higher early constitutive immune defenses than

402 expected by metabolic rates. B and T cell receptor diversity is more constrained by over-
403 responsiveness to self- than under-responsiveness to non-self (De Boer and Perelson 1993).
404 Indeed, the probability that a parasite will evade the antigen space covered by B and T cell
405 repertoires is $4x10^{-44}$ (Perelson and Oster 1979; Banerjee et al. 2017). Adaptive immune systems
406 will, therefore, eventually detect any antigen that ever evolves. The challenge of relying solely
407 on these defenses, though, is that they involve major time lags (i.e., minimally 4-10 days but
408 perhaps longer if the immune system is still developing (Ricklefs 1992). Lags for inducible
409 defenses generally leave hosts vulnerable as microbial doubling time proceeds over a much
410 shorter period. This incompatibility might explain why among 25 avian species, the production
411 rate of infectious virions and the burst size of cells (i.e., the number of infectious virions released
412 by an infected cell over its infected lifespan) scaled hypometrically, yet the rate of antibody-
413 mediated neutralization of virus was isometric (Banerjee et al. 2017). Perhaps isometrically-
414 scaled constitutive immune defenses produced the surprisingly low viral outcomes observed in
415 that study.

416 If considered more broadly, our results might in fact be consistent with the Safety Factory
417 Hypothesis. Perhaps instead of predicting hypermetric scaling of all forms of constitutive innate
418 immunity, the Safety Factory Hypothesis should instead posit that large and small animals need
419 equal *functional* protection against pathogens resulting in hypermetric scaling of some defenses
420 and isometric (or even hypometric) scaling of others. Large mammals (Downs et al. 2020) and
421 large birds (Ruhs et al. 2020) have disproportionally higher concentrations of early responding
422 granulocytes relative to their small counterparts. However, this hypermetric scaling may not
423 translate into hypermetric scaling of functionally because the synthesis of immunological
424 molecules and cellular rates of reaction might be constrained by metabolic rate (Brown et al.

425 2004; Savage et al. 2007). In other words, the disproportionately high concentrations of
426 granulocytes in large species might be necessary to have similar functionality as small species
427 (Downs et al. 2020; Ruhs et al. 2020). Large animals may use a strategy of many cells with
428 reduced activity, whereas small animals may use a strategy of fewer cells with higher activity.
429 To test further test this idea, we would need to determine the scaling coefficient for the
430 functionality of neutrophils and the scaling of the number of hepatocytes that produce
431 complement and their functionality.

432 Phylogenetic signal and other influences on antibacterial capacity

433 Our results also demonstrated that mammals exhibit a high diversity of antibacterial
434 curves (Movie S1) and that little of this variation is explained by phylogeny or body size. The
435 weak phylogenetic signal and a small percentage of variation in antibacterial curves explained by
436 phylogeny in general were surprising. Previous analyses of scaling of leucocyte concentrations
437 and in mammals (Downs et al. 2020) and birds (Ruhs et al. 2020) and leucocyte ratios in birds
438 (Minias 2019) demonstrated that phylogeny explained the majority of interspecific variation.
439 Although phylogenetic signal was weak for many aspects of antibacterial capacity we measured,
440 we caution against equating a lack of signal with a lack of phylogenetic effect (Blomberg and
441 Garland 2002),. Our statistics were not designed to test the coevolution of these traits over time,
442 rather they look for phylogenetic covariances in the extant traits

443 Life history, diet, and other differences may also explain some variation in antibacterial
444 capacity curves among mammalian species. The pace-of-life hypothesis posits that reproductive
445 rate and longevity, among other life-history traits, should shape investment in immune defenses
446 (Lee 2006). Although life histories are closely tied to body mass in mammals (Peters 1983;
447 Calder 1984), species of the same mass, but with different life histories, will have different costs

448 and benefit structures for immune defense. For example, small species that are relatively long-
449 lived incur the higher costs of activating immune responses (Brace et al. 2017), natural antibody
450 titers increased with incubation period in 70 species of tropical birds after accounting for body
451 mass statistically (Lee et al. 2008), and faster-lived birds produced more of an acute-phase
452 protein after inoculation with *E. coli* after accounting for body mass (Robinson et al. 2010).
453 Determining if life history explains the residual variation after accounting for body mass and
454 phylogeny is a next step towards understanding the variation in interspecific variation in
455 antibacterial capacity, but are beyond the scope of theis current study
456

457 **Conclusion**

458 Our findings suggest that large and small species might use different strategies to obtain
459 the same level of protection against parasites. They have ramifications for human medicine and
460 management of disease cycles, especially zoonoses, and a greater understanding of immune
461 scaling could also help improve epidemiological models. A previously developed allometric
462 framework for host-species competence for multi-host parasites found that data on interspecific
463 allometries of immune defenses was lacking in the literature (Downs et al. 2019). Because "the
464 rate that pathogens spread through populations is influenced by the rate of spread through
465 individual hosts" (De Leo and Dobson 1996), we must understand better how host traits affect
466 their propensity to maintain and transmit viable parasites (Bolzoni et al. 2008; De Leo et al.
467 2016).

468 We expect that many more important immune allometries await description. In particular,
469 we encourage future scaling work on Order *Chiroptera*, as bats are implicated in the emergence
470 of many zoonoses including SARS-COV2 (Han et al. 2016; Olival et al. 2017). Unfortunately,

471 bats are rare in zoos, so few bat species were in the present analysis (but see Ruhs et al. In press).
472 We also encourage efforts to investigate immune allometries in ectotherms, and especially
473 vectors, as their immune defenses are more temperature-dependent than mammals (Brown et al.
474 2004), an important condition for a planet undergoing extensive climate change. We also hope
475 creative approaches can be applied to scaling studies of more pathogenic microbes, ideally in
476 more organismal contexts. Such work is challenging, as pathogenicity differs among species as
477 well as route of infection (Taylor 1983). By continuing to merge cellular and molecular efforts
478 with the behavioral, ecological, and evolutionary concepts, we can produce a more integrative
479 immunology and thus more effective options to predict and manage infectious disease risk.
480

481 **Author Contributions:** C.J.D., L.B.M, and K.C.K. conceptualized the study; L.A.S., S.J.O. and
482 C.J.D., and R.B. procured samples; L.A.S., S.J.O. and C.J.D. established and validated the
483 laboratory methodology; L.A.S., S.J.O., C.J.D., and L.B.M collected and curated the data; C.J.D.
484 carried out the formal analysis with input from L.B.M and E.W.G; C.J.D and L.B.M drafted the
485 manuscript with input from K.C.K; all authors contributed to writing and revision; C.J.D and
486 L.B.M. administered and supervised the project; C.J.D., L.B.M., and R.H.Y.J acquired funding.
487

488 **Acknowledgements:** We thank Birmingham Zoo, Busch Gardens Tampa Bay (Cara Martel),
489 Cleveland Metroparks Zoo, Columbus Zoo, the Denver Zoological Foundation, Dickerson Park
490 Zoo, Indianapolis Zoo, Lincoln Park Zoo, Louisville Zoological Garden, Maryland Zoo in
491 Baltimore, Milwaukee County Zoo, Naples Zoo, Nashville Zoo at Grassmere, Oregon Zoo
492 (Mitch Finegan & David Shepherdson), Sedgwick County Zoo, Smithsonian's National Zoo and
493 Conservation Biological Institute, Topeka Zoo & Conservation Center, Zoo Atlanta (Hayley

Murphy, Stephanie Earhardt), ZooTampa at Lowry Park, and the Demas (Indiana State University), Hoekstra (Harvard University), Ophir (Cornell University), Place (Cornell University), and Monteith (University of Wyoming) labs for donating serum samples. We thank M. Amy, B. Butler, K. Carlson, E. Chinchilli, K. Clausen, H. Droke, M. Espino, A. Fernandez, M. Galan, M. Henning, N. Huizenga, K. Koller, E. Lee, O. Ogunsina, V. Pappademetriou, A. Roberts, C. Stanell, S. Travis, A. Vorrath, R. Winner, C. Yeung for help with laboratory work. N. Keith helped develop the Program R workflows required to process our data. We thank N.A. Dochtermann and J.C. Uyeda for statistical guidance, and the Martin Lab, HA Woods, J.F. Harrison, ME Sobolewski, and V Savage for discussion about an early version of the manuscript. This work was supported by State University of New York College of Environmental Science and Forestry's Provost Office, the Levitt Center, Hamilton College's Dean of Faculty Office, University of South Florida's College of Public Health, and the National Science Foundation (award numbers IOS 1656551 to C.J.D. and IOS 1656618 to L.B.M).

Data Accessibility: The datasets generated during and/or analyzed during the current study and will be deposited in Figshare after a 3-year embargo. We will consider written requests for the data prior to the end of the embargo. Lab protocols (Schoenle et al. 2020) and R code (Keith et al. 2020; Downs et al. 2021) are available on FigShare.

References

Banerjee, S. 2018. A mathematical framework for understanding how lymph node architecture scales with host body size to produce an efficient immune response 8.

Banerjee, S., and M. Moses. 2010. Scale Invariance of Immune System Response Rates and Times: Perspectives on Immune System Architecture and Implications for Artificial Immune Systems. arXiv:1008.1380 [cs, math, q-bio].

Banerjee, S., and M. E. Moses. 2009. A Hybrid Agent Based and Differential Equation Model of Body Size Effects on Pathogen Replication and Immune System Response. Pages 14–18 *in* P. S. Andrews, J. Timmis, N. D. L. Owens,

U. Aickelin, E. Hart, A. Hone, and A. M. Tyrrell, eds. Artificial Immune Systems (Vol. 5666). Springer Berlin Heidelberg, Berlin, Heidelberg.

Banerjee, S., A. S. Perelson, and M. Moses. 2017. Modelling the effects of phylogeny and body size on within-host pathogen replication and immune response. Journal of The Royal Society Interface 14:20170479.

Bennett, A. F., and R. B. Huey. 1990. Studying the evolution of physiological performance. Oxford surveys in evolutionary biology 7:251–284.

Blomberg, S. P., and T. Garland. 2002. Tempo and mode in evolution: phylogenetic inertia, adaptation and comparative methods: Phylogenetic inertia. Journal of Evolutionary Biology 15:899–910.

Blount, J. D., D. C. Houston, A. P. Moller, and J. Wright. 2003. Do individual branches of immune defence correlate? A comparative case study of scavenging and non-scavenging birds. Oikos 102:340–350.

Bolzoni, L., G. A. De Leo, M. Gatto, and A. P. Dobson. 2008. Body-size scaling in an SEI model of wildlife diseases. Theoretical Population Biology 73:374–382.

Brace, A. J., M. J. Lajeunesse, D. R. Ardia, D. M. Hawley, J. S. Adelman, K. L. Buchanan, J. M. Fair, et al. 2017. Costs of immune responses are related to host body size and lifespan. Journal of Experimental Zoology Part A: Ecological and Integrative Physiology 327:254–261.

Brown, J. H., J. F. Gillooly, A. P. Allen, V. M. Savage, and G. B. West. 2004. Toward a Metabolic Theory of Ecology. Ecology 85:1771–1789.

Calder, W. A., III. 1984. Size, function, and life history. Dover Publications, Mineola, NY.

Commo, F., and B. M. Bot. 2016. R package nplr n-parameter logistic regressions 11.

De Boer, R. J., and A. S. Perelson. 1993. How diverse should the immune system be? Proceedings of the Royal Society of London. Series B: Biological Sciences 252:171–175.

De Leo, G. A., and A. P. Dobson. 1996. Allometry and simple epidemic models for microparaites. Nature 379:720–722.

De Leo, G. A., A. P. Dobson, and M. Gatto. 2016. Body size and meta-community structure: the allometric scaling of parasitic worm communities in their mammalian hosts. Parasitology 143:880–893.

de Villemereuil, P., and S. Nakagawa. 2014. General Quantitative Genetic Methods for Comparative Biology. Pages 287–303 *in* L. Z. Garamszegi, ed. Modern Phylogenetic Comparative Methods and Their Application in Evolutionary Biology. Springer Berlin Heidelberg, Berlin, Heidelberg.

Demas, G. E., D. A. Zysling, B. R. Beechler, M. P. Muehlenbein, and S. S. French. 2011. Beyond phytohaemagglutinin: assessing vertebrate immune function across ecological contexts: Assessing vertebrate immune function across ecological contexts. Journal of Animal Ecology 80:710–730.

Diamond, J. 2002. Quantitative evolutionary design. The Journal of Physiology 542:337–345.

Dingemanse, N. J., and N. A. Dochtermann. 2013. Quantifying individual variation in behaviour: mixed-effect modelling approaches. (M. van de Pol, ed.)Journal of Animal Ecology 82:39–54.

Dingli, D., and J. M. Pacheco. 2006. Allometric Scaling of the Active Hematopoietic Stem Cell Pool across Mammals. (C. Arendt, ed.)PLoS ONE 1:e2.

Dobson, A. P., and P. J. Hudson. 1986. Parasites, disease and the structure of ecological communities. Trends in Ecology & Evolution 1:11–15.

Downs, C. J., J. S. Adelman, and G. E. Demas. 2014. Mechanisms and Methods in Ecoimmunology: Integrating Within-Organism and Between-Organism Processes. Integrative and Comparative Biology 54:340–352.

Downs, C. J., N. A. Dochtermann, R. Ball, K. C. Klasing, and L. B. Martin. 2020. The Effects of Body Mass on Immune Cell Concentrations of Mammals. American Naturalist 195:107–114.

Downs, C. J., E. W. Goolsby, and L. B. Martin. 2021. Rphylopars code for comparative antimicrobial analysis. FigShare. DOI:10.6084/m9.figshare.14806962

Downs, C. J., L. A. Schoenle, B. A. Han, J. F. Harrison, and L. B. Martin. 2019. Scaling of Host Competence. Trends in Parasitology 35:182–192.

Ezenwa, V. O. 2004. Interactions among host diet, nutritional status and gastrointestinal parasite infection in wild bovids. International Journal for Parasitology 34:535–542.

Fassbinder-Orth, C. A., L. D. Igl, D. C. Hahn, K. M. Watts, T. E. Wilcoxen, and K. R. Ramos-Álvarez. 2019. Do Life History Traits Influence Patterns of Maternal Immune Elements in New World Blackbirds (Icteridae)? Integrative Organismal Biology 1.

Felsenstein, J. 1985. Phylogenies and the Comparative Method. The American Naturalist 125:1–15.

Filion, A., A. Eriksson, F. Jorge, C. N. Niebuhr, and R. Poulin. 2020. Large-scale disease patterns explained by climatic seasonality and host traits. Oecologia.

French, S. S., and L. A. Neuman-Lee. 2012. Improved ex vivo method for microbiocidal activity across vertebrate species. Biology Open 1:482–487.

Garamszegi, L. Z. 2014. Uncertainties Due to Within-Species Variation in Comparative Studies: Measurement Errors and Statistical Weights. Pages 157–199 *in* L. Z. Garamszegi, ed. Modern Phylogenetic Comparative Methods and Their Application in Evolutionary Biology: Concepts and Practice. Springer Berlin Heidelberg, Berlin, Heidelberg.

Garamszegi, L. Z., and A. P. Møller. 2010. Effects of sample size and intraspecific variation in phylogenetic comparative studies: a meta-analytic review. Biological Reviews no-no.

Goolsby, E. W., J. Bruggeman, and C. Ané. 2017. Rphylopars : fast multivariate phylogenetic comparative methods for missing data and within-species variation. (R. Fitzjohn, ed.)Methods in Ecology and Evolution 8:22–27.

Goolsby, E. W., J. Bruggeman, and C. Ane. 2021. Rphylopars: Phylogenetic Comparative Tools for Missing Data and Within-Species Variation.

Hadfield, J. D. 2010. MCMC Methods for Multi-Response Generalized Linear Mixed Models: The **MCMCglmm** *R* Package. Journal of Statistical Software 33.

Hadfield, J. D., and S. Nakagawa. 2010. General quantitative genetic methods for comparative biology: phylogenies, taxonomies and multi-trait models for continuous and categorical characters. Journal of Evolutionary Biology 23:494–508.

Han, B. A., A. M. Kramer, and J. M. Drake. 2016. Global Patterns of Zoonotic Disease in Mammals. Trends in Parasitology 32:565–577.

Harrison, J. F. 2017. Do Performance–Safety Tradeoffs Cause Hypometric Metabolic Scaling in Animals? Trends in Ecology & Evolution 32:653–664.

Harrison, L. 1915. Mallophaga from *Apteryx* , and their Significance; with a Note on the Genus *Rallicola*. Parasitology 8:88–100.

Ishtiaq, F., C. G. R. Bowden, and Y. V. Jhala. 2017. Seasonal dynamics in mosquito abundance and temperature do not influence avian malaria prevalence in the Himalayan foothills. Ecology and Evolution 7:8040–8057.

Keith, N. I., L. B. Martin, and C. J. Downs. 2020. Code to compile data and analyzing data for a comparative antimicrobial analysis. figshare. DOI: 10.6084/m9.figshare.12430103

Kelt, D. A., and D. H. Van Vuren. 2001. The Ecology and Macroecology of Mammalian Home Range Area. The American Naturalist 157:637–645.

Kieft, T. L., and K. A. Simmons. 2015. Allometry of animal–microbe interactions and global census of animal-associated microbes. Proceedings of the Royal Society B: Biological Sciences 282:20150702.

Kuris, A. M., A. R. Blaustein, and J. J. Alio. 1980. Hosts as islands. American Naturlists 116:570–586.

Langman, R. E., and M. Cohn. 1987. The E-T (Elephant-Tadpole) paradox necessitates the concept of a unity of B-cell function: The protecton. Molecular Immunology 24:675–697.

Lee, K. A. 2006. Linking immune defenses and life history at the levels of the individual and the species. Integrative and Comparative Biology 46:1000–1015.

Lee, K. A., M. Wikelski, W. D. Robinson, T. R. Robinson, and K. C. Klasing. 2008. Constitutive Immune Defences Correlate with Life-History Variables in Tropical Birds. Journal of Animal Ecology 77:356–363.

Letunic, I. 2015. phyloT: phylogenetic tree generator

Lindstedt, S. L., B. J. Miller, and S. W. Buskirk. 1986. Home Range, Time, and Body Size in Mammals. Ecology 67:413–418.

Lubbers, R., M. F. van Essen, C. van Kooten, and L. A. Trouw. 2017. Production of complement components by cells of the immune system: Production of complement components. Clinical & Experimental Immunology 188:183–194.

Mastroeni, P., J. A. Chabalgoity, S. J. Dunstan, D. J. Maskell, and G. Dougan. 2001. Salmonella: Immune Responses and Vaccines. The Veterinary Journal 161:132–164.

Minias, P. 2019. Evolution of heterophil/lymphocyte ratios in response to ecological and life-history traits: A comparative analysis across the avian tree of life. (D. Ardia, ed.)Journal of Animal Ecology 88:554–565.

Mittrücker, H.-W., and S. H. E. Kaufmann. 2000. Immune response to infection with *Salmonella typhimurium* in mice. Journal of Leukocyte Biology 67:457–463.

Murphy, K. P., P. Travers, and M. Walport. 2007. Janeway's immunobiology. (7th ed.). Garland Science, New York.

Nagy, K. A. 2001. Food requirements of wild animals: predictive equations for free-living mammals, reptiles, and birds. Nutrition Abstracts and Reviews, Series B 71:21R-31R.

Nunn, C. L. 2002. A COMPARATIVE STUDY OF LEUKOCYTE COUNTS AND DISEASE RISK IN PRIMATES. Evolution 56:177–190.

Nunn, C. L., J. L. Gittleman, and J. Antonovics. 2003. A comparative study of white blood cell counts and disease risk in carnivores. Proceedings of the Royal Society of London. Series B: Biological Sciences 270:347–356.

Olival, K. J., P. R. Hosseini, C. Zambrana-Torrelio, N. Ross, T. L. Bogich, and P. Daszak. 2017. Host and viral traits predict zoonotic spillover from mammals. Nature 546:646–650.

Pagel, M. 1997. Inferring evolutionary processes from phylogenies. Zoologica Scripta 26:331–348.

———. 1999. Inferring the historical patterns of biological evolution. Nature 401:877–884.

Perelson, A. S., and G. Oster. 1979. Theoretical Studies of Clonal Selection: Minimal Antibody Repertoire Size and Reliability of Self-Non-self Discriminationt. Journal of Theoretical Biology 81:645–670.

Peters, R. H. 1983. The ecological implications of body size. Cambridge University Press, New York.

Peto, R. 1977. Epidemiology, multistage models, and short-term mutagenicity tests. Pages 1403–1428 *in* J. D. Watson, H. H. Hiatt, and J. A. Winsten, eds. Origins of human cancer. Cold Spring Harbor Laboratory, New York, NY.

Poulin, R. 2007. Evolutionary ecology of parasites. Princeton University Press, Princeton, NJ.

Poulin, R., and M. George-Nascimento. 2007. The scaling of total parasite biomass with host body mass. International Journal for Parasitology 37:359–364.

Prothero, J. W. 2015. The Design of Mammals: A Scaling Approach. Cambridge University Press, Cambridge.

R Core Team. 2019. R: A language and environment for statistical computing. R Foundation for Statistical Computing, Vienna, Austria.

Ricklefs, R. E. 1992. Embryonic development period and the prevalence of avian blood parasites. Proceedings of the National Academy of Sciences 89:4722–4725.

Robinson, W. D., M. Hau, K. C. Klasing, M. Wikelski, J. D. Brawn, S. H. Austin, C. Tarwater, et al. 2010. Diversification of Life Histories in New World Birds. The Auk 127:253–262.

652 Ruhs, E. C., D. J. Becker, S. J. Oakey, O. Ogunsina, M. B. Fenton, Simmons, Nancy B., L. B. Martin, et al. In press.
653 Body size affects immune cell proportions in birds and non-volant mammals, but not bats. Journal of Experimental
654 Biology.

655 Ruhs, E. C., L. B. Martin, and C. J. Downs. 2020. The impact of body mass on immune cell concentrations in birds.
656 Proceedings of the Royal Society B: Biological Sciences 287:20200655.

657 Savage, V. M., A. P. Allen, J. H. Brown, J. F. Gillooly, A. B. Herman, W. H. Woodruff, and G. B. West. 2007.
658 Scaling of number, size, and metabolic rate of cells with body size in mammals. Proceedings of the National
659 Academy of Sciences 104:4718–4723.

660 Savage, V. M., J. F. Gillooly, W. H. Woodruff, G. B. West, A. P. Allen, B. J. Enquist, and J. H. Brown. 2004. The
661 predominance of quarter-power scaling in biology. Functional Ecology 18:257–282.

662 Schmidt-Nielsen, K. 1984. Scaling: why is animal size so important? Cambridge University Press, Cambridge.

663 Schneeberger, K., G. Á. Czirják, and C. C. Voigt. 2013. Measures of the Constitutive Immune System Are Linked to
664 Diet and Roosting Habits of Neotropical Bats. (J. D. Brown, ed.)PLoS ONE 8:e54023.

665 Schoenle, L. A., C. J. Downs, and L. B. Martin. 2018. An Introduction to Ecoimmunology. Pages 901–932 *in* E. L.
666 Cooper, ed. Advances in Comparative Immunology. Springer International Publishing, Cham.

667 Schoenle, L. A., L. B. Martin, and C. J. Downs. 2020. Protocols for 12-dilution antibacterial capacity curves for
668 interspecific comparisons. Figshare. DOI: 10.6084/m9.figshare.12501149

669 Sears, M. W., J. P. Hayes, C. S. O'Connor, K. Geluso, and J. S. Sedinger. 2006. Individual variation in thermogenic
670 capacity affects above-ground activity of high-altitude Deer Mice. Functional Ecology 20:97–104.

671 Sheldon, B. C., and S. Verhulst. 1996. Ecological immunology: costly parasite defences and trade-offs in
672 evolutionary ecology. Trends in Ecology & Evolution 11:317–321.

673 Shudo, E., and Y. Iwasa. 2001. Inducible Defense against Pathogens and Parasites: Optimal Choice among Multiple
674 Options. Journal of Theoretical Biology 209:233–247.

675 Sieg, A. E., M. P. O'Connor, J. N. McNair, B. W. Grant, S. J. Agosta, and A. E. Dunham. 2009. Mammalian
676 Metabolic Allometry: Do Intraspecific Variation, Phylogeny, and Regression Models Matter? The American
677 Naturalist 174:720–733.

678 Smith, F. A., and S. K. Lyons. 2011. How big should a mammal be? A macroecological look at mammalian body
679 size over space and time. Philosophical Transactions of the Royal Society B: Biological Sciences 366:2364–2378.

680 Taylor, P. W. 1983. Bactericidal and bacteriolytic activity of serum against gram-negative bacteria. Microbiological
681 Reviews 47:46–83.

682 Tian, J., A. Courtiol, K. Schneeberger, A. D. Greenwood, and G. Á. Czirják. 2015. Circulating white blood cell
683 counts in captive and wild rodents are influenced by body mass rather than testes mass, a correlate of mating
684 promiscuity. (T. Piersma, ed.)Functional Ecology 29:823–829.

685 Tough, D. F., and J. Sprent. 1995. Lifespan of lymphocytes. Immunologic Research 14:1–12.

686 Uyeda, J. C., M. W. Pennell, E. T. Miller, R. Maia, and C. R. McClain. 2017. The Evolution of Energetic Scaling
687 across the Vertebrate Tree of Life. The American Naturalist 190:185–199.

688 van der Poll, T., and S. M. Opal. 2008. Host–pathogen interactions in sepsis. The Lancet Infectious Diseases 8:32–
689 43.

690 Wiegel, F. W., and A. S. Perelson. 2004. Some Scaling Principles for the Immune System. Immunology and Cell
691 Biology 82:127–131.

692

693 **Table 1.** Covariance (Mean ± 95% CI) between body mass and antibacterial capacity curve

694 parameters from phylogenetic covariance models estimated using the `Rphylopars` in Program

695 R.

Antibacterial capacity curve parameter	Estimate of covariance by dataset		
	E. coli	***S. enterica***	***M. luteus***
Top asymptote[#]	-0.002 (-0.036 : 0.035)	N/A*	-0.024 (-0.113 : 0.064)
Slope	9.50 (-4.3 : 26.3)	-0.394 (-11.9 : 12.6)	-11.0 (-22.8 : -2.6)
$\text{Inflection}_{\text{dilution}}$	-0.262 (-0.723 : 0.360)	-0.126 (-0.747 : 0.465)	-0.103 (-0.954 : 0.947)
Asymptote coefficient	-0.022 (-0.345 : 0.178)	-0.107 (-0.341 : 0.033)	-0.022 (-0.390 : 0.156)
$\text{Inflection}_{\text{antibacterial capacity}}$	-0.006 (-0.284 : 0.036)	0.009 (-0.146 : 0.445)	-0.023 (-0.087 : 4.47)
Bottom asymptote	-0.002 ($-1.3 \times 10^{78} : 2.1 \times 10^{95}$)	-0.009 (-0.409 : 0.046)	-0.041 ($-2.0 \times 10^{33} : 3.61$)

696

697 [#] $\text{Inflection}_{\text{antibacterial capacity}}$, top asymptote, and bottom asymptote were +1, $\log_{10}$-transformed. Body mass and slope

698 were $\log_{10}$-transformed prior to beta estimation.

699 * Top asymptote was not included in the model for antibacterial capacity against *S. enterica* because it was highly

700 correlated (r = 0.998) with $\text{Inflection}_{\text{antibacterial capacity}}$. Both variables could not be included in the same model

701

702 **Table 3.** Estimates of the percent of variation in antibacterial curves against *E. coil*, *S. enterica,*

703 and *M. luteus* explained by phylogeny from phylogenetic covariance models estimated using the

704 `Rphylopars` in Program R.

	Lambda (P-value)			**Variance explained (%)**		
Antibacterial capacity curve parameter	***E. coli***	***S. enterica***	***M. luteus***	***E. coli***	***S. enterica***	***M. luteus***
Body mass*	**1 (<0.001)**	**1 (<0.001)**	**1 (<0.001)**	98.0	97.5	97.5
Top asymptote	0.008 (1)	N/A	0.179 (0.449)	11.6	N/A	24.6
Slope	**0.971 (<0.001)**	0.996 (0.137)	0.445 (0.016)	28.1	5.47	17.0
$\text{Inflection}_{\text{antibacterial capacity}}$	0.075 (0.984)	0.474 (0.363)	0.221 (0.249)	10.7	30.0	23.4
$\text{Inflection}_{\text{dilution}}$	**0.996 (0.002)**	**0.999 (<0.001)**	**0.998 (0.004)**	20.2	54.2	16.4
Asymptote coefficient	0.753 (0.378)	0.358 (0.492)	0.198 (0.872)	3.8	3.7	7.1
Bottom asymptote	**0.976 (<0.001)**	0.431 (0.162)	0.003 (1)	31.1	18.8	10.6

705 * $\text{Inflection}_{\text{antibacterial capacity}}$, top asymptote, and bottom asymptote were +1, $\log_{10}$-transformed. Body mass and slope

706 were $\log_{10}$-transformed prior to beta estimation.

707

708 **Table 3.** Estimated intercepts and scaling coefficients (mode ± 95% CI) for curve parameters of
709 antibacterial capacity against *E. coli, S. enterica, M. luteus* from phylogenetic univariate mixed
710 effects models. Estimates in **bold** have 95% CI intervals that do not overlap 0.
711

	Fixed effect: log_{10} body mass					
	Intercept			**Slope**		
Antibacterial capacity curve parameter	**Beta estimate**	**Effective sample**	**pMCMC**	**Beta estimate**	**Effective sample**	**pMCMC**
E. coli						
$Inflection_{antibacterial\ capacity*}$	**-0.876 (-1.331 : -0.521)**	**1000**	**<0.001**	-0.033 (-0.144 : 0.044)	1000	0.278
Slope	**42.4 (26.8 : 57.9)**	**1000**	**<0.001**	0.984 (-3.257 : 3.89)	1000	0.828
Top asymptote	**0.266 (0.199 : 0.343)**	**1102**	**<0.001**	0.008 (-0.007 : 0.026)	1000	0.26
$Inflection_{dilution}$	**0.179 (0.107 : 0.253)**	**1000**	**<0.001**	0.006 (-0.011 : 0.021)	1124	0.514
Bottom asymptote	**0.062 (0.009 : 0.113)**	**1000**	**0.044**	-0.004 (-0.018 : 0.007)	1093	0.362
Asymmetric coefficient	**16.5 (6.7 : 25.1)**	**1000**	**<0.001**	-0.675 (-2.541 : 1.495)	1000	0.62
S. enterica						
$Inflection_{antibacterial\ capacity}$	**-0.905 (-1.296 : -0.557)**	**886.9**	**<0.001**	-0.027 (-0.102 : 0.061)	887.4	0.754
Slope	**34.6 (15.4 : 49.8)**	**901.8**	**<0.001**	-0.376 (-4.42 : 3.479)	898.3	0.648

Top asymptote	**0.311** **(0.205 : 0.41)**	**1000**	**<0.001**	0.008 (-0.019 : 0.028)	1000	0.72
Inflection$_{dilution}$	**0.218** **(0.134 : 0.324)**	**1000**	**<0.001**	-0.004 (-0.019 : 0.022)	1000	0.982
Bottom asymptote	0.02 (-0.047 : 0.085)	1225.3	0.51	-0.007 (-0.019 : 0.01)	1220.6	0.502
Asymmetric coefficient	**24.5** **(13.1 : 34.3)**	**1000**	**<0.001**	**-3.778** **(-5.604 : -0.907)**	**1000**	**<0.001**
M. luteus						
Inflection$_{antibacterial\ capacity}$	-0.727 (-2.029 : 0.565)	1000	0.302	-0.112 (-0.401 : 0.177)	1000	0.412
Slope	**33.2** **(14.8 : 46.8)**	**1000**	**<0.001**	**-4.309** **(-7.652 : -0.788)**	**1000**	**0.018**
Top asymptote	**0.26** **(0.097 : 0.414)**	**1000**	**<0.001**	0.016 (-0.018 : 0.052)	1000	0.306
Inflection$_{dilution}$	**0.178** **(0.062 : 0.327)**	**1000**	**0.004**	0.006 (-0.017 : 0.042)	1000	0.382
Bottom asymptote	0.074 (-0.025 : 0.282)	1000	0.108	-0.029 (-0.067 : 0.004)	1112	0.112
Asymmetric coefficient	4.8 (-13.2 : 17.7)	1097	0.778	1.967 (-1.652 : 4.864)	1117	0.37

712 * Inflection$_{antibacterial\ capacity,}$ top asymptote, and bottom asymptote were +1, log_{10}-transformed. Body mass and slope

713 were log_{10}-transformed prior to beta estimation.

714

Figures

Figure 1. Antibacterial capacity dilution curves support the Safety Factor Hypothesis. Hypothetical antibacterial dilution curve showing the parameters we estimated and biological interpretation (A) This curve shows, names (underlined), and described the curve parameters and the biological interpretation of the curve parameter (in bold). Hypothetical antibacterial curves for an elephant and mouse showing predictions for the Safety Factory Hypothesis (B), the Rate of Metabolism Hypothesis (C), and the Protecton and Complexity Hypotheses (D).

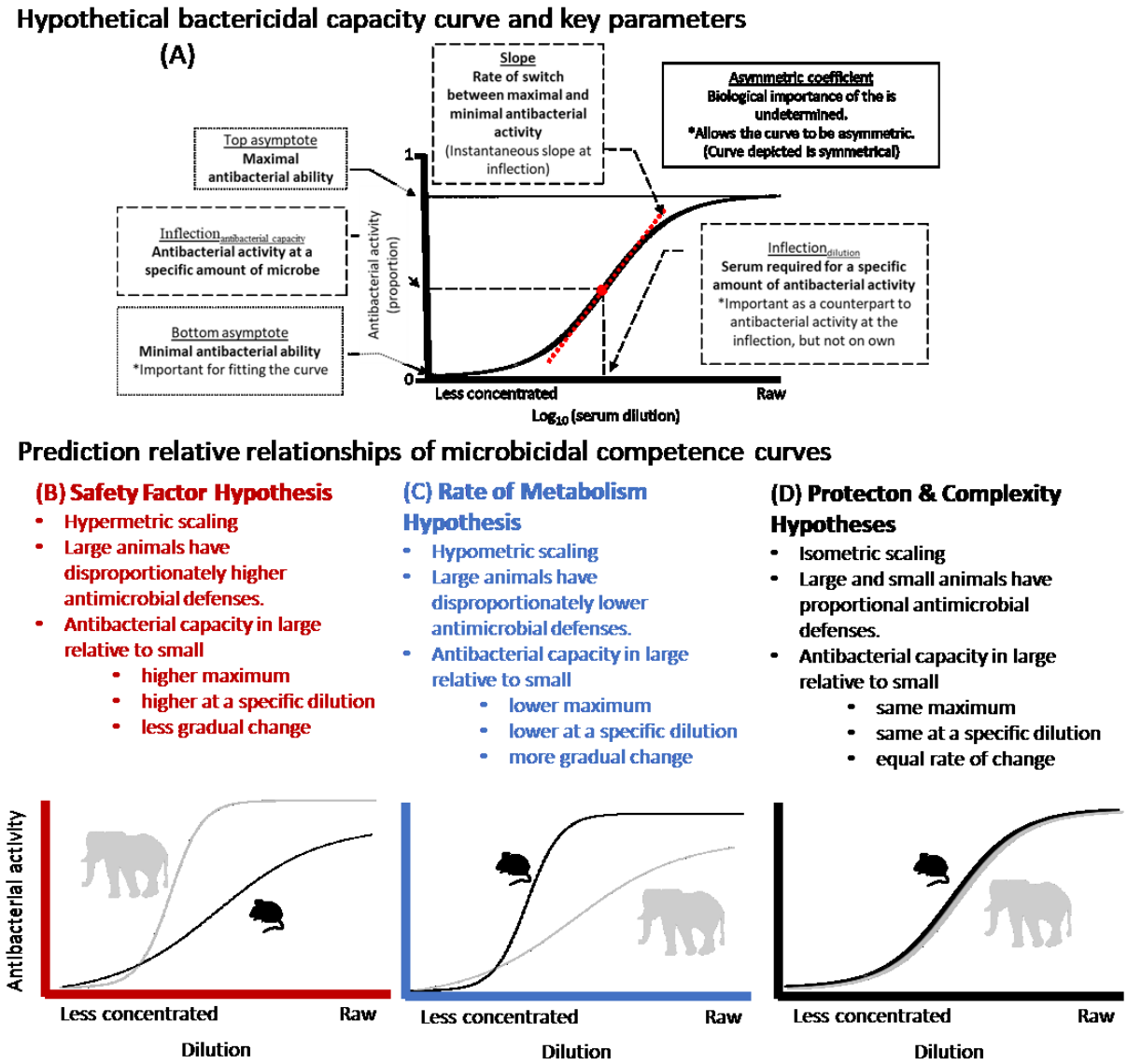
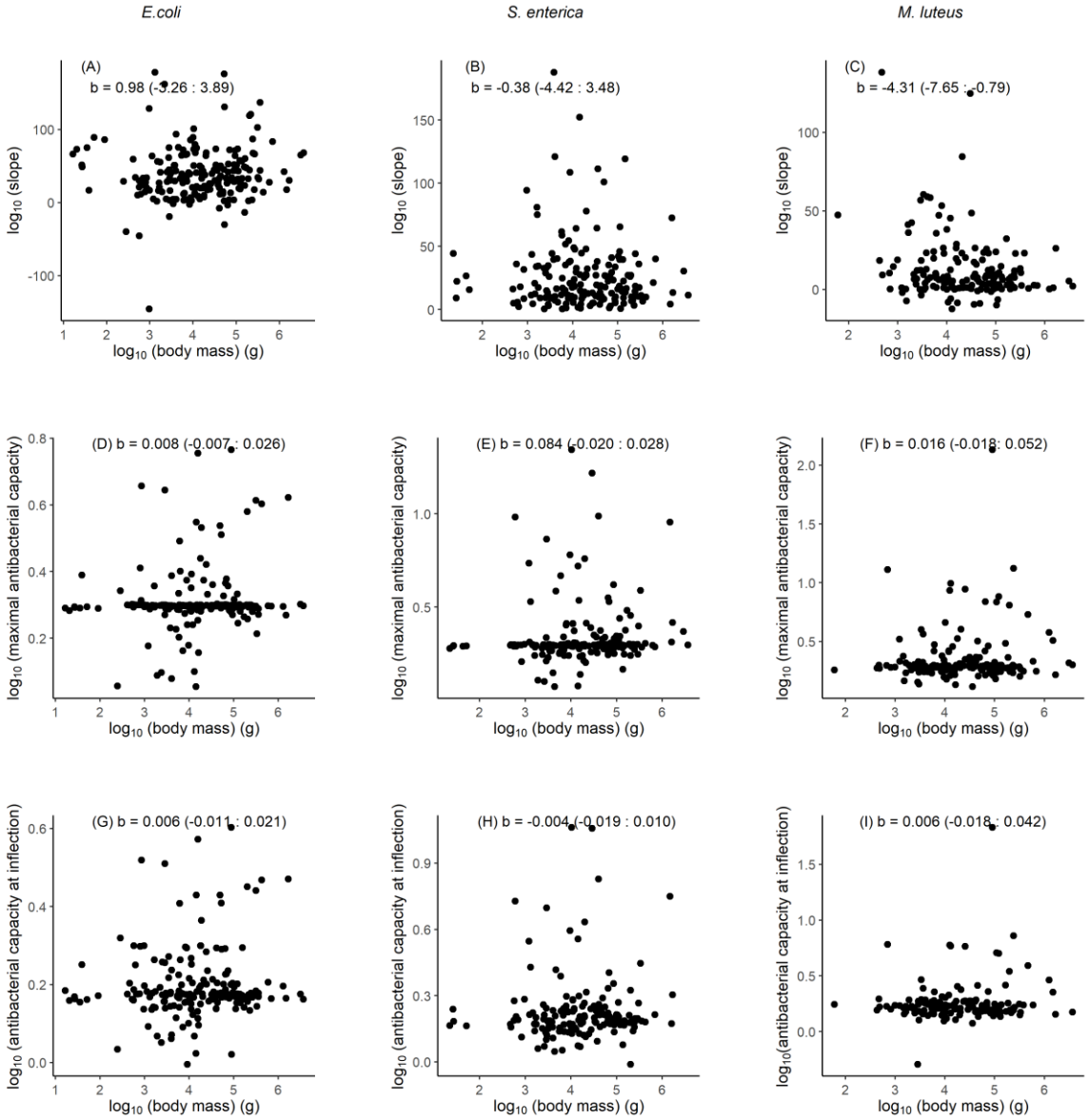
Figure 2. Parameters of antibacterial capacity curves—instantaneous slope at the inflection point (A-C) maximal antibiotic capacity (D-F), and antibiotic capacity at the inflection point (G-I)—against *Escherichia coli* (A, D, G,), *Salmonella enterica* (B, E, H), *Micrococcus luteus* and (C, F, I) against body mass. Each point represents a species mean, but analyses were performed on individual-level data.